ISSN 1063-7710, Acoustical Physics, 2010, Vol. 56, No. 6, pp. 877–892. © Pleiades Publishing, Ltd., 2010.

Love Waves in Nondestructive Diagnostics of Layered Composites. Survey

S. V. Kuznetsov

Institute for Problems in Mechanics, Russian Academy of Sciences, pr. Vernadskogo 101, Moscow, 119526 Russia
e-mail: svkuznec@ipmnet.ru

Received March 19, 2010

Abstract—A survey of application of surface acoustic waves for nondestructive diagnostics of layered media is presented. A mathematical model for description of propagation of surface acoustic Love waves in layered anisotropic nanocomposites based on the modified transfer matrix method is constructed. Dispersion relations for media consisting of one and two elastically anisotropic layers in contact with the anisotropic half-space are analyzed. Waves with horizontal transverse polarization of noncanonical type are considered.

DOI: 10.1134/S1063771010060126

1. INTRODUCTION

1.1. Modern State of the Problem

The growing needs of microelectronics and other fields of modern technology require introduction and development of methods of nondestructive analysis of multilayered materials. The basis of these methods is acoustic waves, thermal waves, or electromagnetic waves, including waves of the X-ray spectrum. Mastering and application of extremely high frequencies in acoustics makes it possible to analyze the properties of very thin layers and internal defects in multilayered materials. Modern acoustic setups provide generation of acoustic waves with frequencies of the order of 1–10 GHz, which makes feasible studies of physical and chemical properties of multilayered structures containing up to five to seven anisotropic layers with a thickness of the order of 0.1–1 μm. Experimental mastering of the frequency range of 0.1–1 THz provides opportunities for investigation of multilayered media containing up to 50 anisotropic layers with a layer thickness of 10–100 nm.

Remark 1.1. Here it should be noted that growth of the frequency of acoustic body waves above 4–5 THz turns out to be impossible due to fundamental considerations. For these frequency values, the wavelengths of acoustic body waves for most materials applied in microelectronics turn out comparable with the distance between neighboring atoms and, therefore, frequencies higher than 4–5 THz are beyond the "cut-off" frequency [1].

Usually the determination of physical and mechanical characteristics of layers in acoustic methods is connected with the measurement of propagation velocities and polarization of acoustic waves. These measurements make it possible to construct dispersion relations connecting the phase velocity of the wave and the frequency. The comparison of experimentally determined dispersion relations with theoretical data provides determination of the properties of internal layers, which cannot be studied using direct methods. Naturally, it is necessary to develop an adequate theoretical method for such analysis.

It is shown below that the available theoretical methods for analysis of propagation of surface waves in layered media are limited by isotropic layers contacting with isotropic half-space for a relatively small number of layers (usually not larger than five) or transversally isotropic or orthotropic layers and similar substrate for one to three layers. There also exists a group of methods connected with the investigation of waves in periodic layered media, but these methods are inapplicable for problems of identification of the properties of separate layers.

At the same time, the needs of modern microelectronics require the development of methods and corresponding numerical algorithms applicable for analysis of propagation of surface waves in systems with 10–20 anisotropic layers in contact with an anisotropic substrate (usually silicon monocrystal serves as the latter). Here, it is reasonable to note that the similar problem occurs in seismology; however, in this case frequencies not higher than 1 kHz are used. In seismology the development of theoretical methods for analysis of propagation of surface waves in systems consisting of a large number of layers is quite topical.

1.2. Basic Types of Surface Waves Used in Nondestructive Diagnostics

The following basic types of surface waves can propagate in elastic layered media: Lamb waves propagating in separate layers which have elliptic polarization in the sagittal plane (plane formed by the normal

to the wave front and the normal to the layer surface); Raleigh waves propagating in the half-space, which have the same polarization as Lamb waves and attenuate in the depth; Stoneley waves propagating at the interface of two contacting half-spaces, which have sagittal elliptic polarization and attenuate in the depth in the half-spaces; and Love waves propagating in the system layer (layers)–contacting half-space the polarization of which is orthogonal to the sagittal plane.

Lamb and Love waves are most important for application in microelectronics because they possess dispersion properties and provide reconstruction of physical and chemical properties of separate layers in multilayered systems using corresponding dispersion curves. Unlike these waves, Raleigh and Stoneley waves are much less applicable for nondestructive diagnostics, since they do not possess dispersion properties.

1.2.1. Love waves. These waves possess horizontal transverse polarization and propagate in the system elastic layer (layers)–half-space. In this case for the wave to exist in the half-space the attenuation condition over the depth should be satisfied. These waves first described in [2] have been intensely studied theoretically [3–5] and experimentally [6–8]. In spite of a relatively simple structure (Love waves consist of one partial wave in the half-space and two partial waves in the layer), a corresponding theory for description of Love waves in an anisotropic layer and anisotropic half-space contacting with it has not been completely developed yet.

The displacement field corresponding to the Love wave can be represented in the form

$$\begin{cases} \mathbf{u}_1(\mathbf{x}) = \mathbf{m}(C_1 e^{-ir\gamma_1 x'} + C_2 e^{ir\gamma_1 x'}) e^{ir(\mathbf{n}\cdot\mathbf{x} - ct)}, \\ \mathbf{u}_2(\mathbf{x}) = \mathbf{m}(C_3 e^{ir\gamma_2 x'}) e^{ir(\mathbf{n}\cdot\mathbf{x} - ct)}, \end{cases} \tag{1.1}$$

where $\mathbf{u}_1$ and $\mathbf{u}_2$ are related to displacements in the layer and the substrate, respectively; $\mathbf{m}$ is the unit amplitude (polarization vector; it is assumed that the vector $\mathbf{m}$ is orthogonal to the sagittal plane formed by the vector $\mathbf{n}$ determining the wave front propagation direction and the unit vector $\mathbf{v}$ normal to the free surface); $x' \equiv \mathbf{v}\cdot\mathbf{x}$ is the transversal (vertical) coordinate, below which it is assumed that it takes negative values in the half-space; r is the wave number; c is the phase velocity; and t is the time. The unknown complex coefficients C_k are determined to a factor from the boundary conditions at the external plane boundary,

$$\mathbf{t}_\mathbf{v}\big|_{x'=h} \equiv \mathbf{v}\cdot\mathbf{C}_1 \cdot\cdot \nabla_\mathbf{x}\mathbf{u}_1 = 0, \tag{1.2}$$

and the contact conditions at the interface ($x' = 0$),

$$\begin{cases} \mathbf{v}\cdot\mathbf{C}_1 \cdot\cdot \nabla_\mathbf{x}\mathbf{u}_1 = \mathbf{v}\cdot\mathbf{C}_2 \cdot\cdot \nabla_\mathbf{x}\mathbf{u}_2, \\ \mathbf{u}_1 = \mathbf{u}_2. \end{cases} \tag{1.3}$$

The parameters γ_k, $k = 1, 2$, in (1.1) correspond to the complex roots of the Christoffel equation, which will be introduced below. In Eqs. (1.2), (1.3) C_k, $k = 1, 2$ are the four-valent elasticity tensors of the layer and the half-space, respectively, and h is the layer thickness.

Remark 1.2. According to representation (1.1), the attenuation in the depth of the half-space is provided by the Christoffel parameter γ_2 with negative imaginary part.

According to [2], the following holds.

Proposition 1.1. (1) Studied waves can occur in an isotropic layer and a half-space contacting with it isotropic if and only if the phase velocity satisfies the condition

$$c_1^T < c < c_2^T, \tag{1.4}$$

where $c_k^T = \sqrt{\dfrac{\mu_k}{\rho_k}}$, $k = 1, 2$, are the velocities of transverse body waves in the layer and the half-space, respectively, and μ_k and ρ_k are the corresponding Lame constants and densities.

(2) The dispersion relation between the phase velocity c and the frequency ω can be represented as

$$\omega = \frac{c}{h}\left(\frac{\rho_1 c^2}{\mu_1} - 1\right)^{-1/2} \times \left(\arctan\left(\frac{\mu_2}{\mu_1}\left(\frac{1 - \dfrac{\rho_2 c^2}{\mu_2}}{\dfrac{\rho_1 c^2}{\mu_1} - 1}\right)^{1/2}\right) + n\pi\right), \quad n = 0, 1, 2, \ldots. \tag{1.5}$$

Corollary 1.

(a) For the fixed frequency ω, there exist a finite number of Love waves propagating with different phase velocities $c \in (c_1^T; c_2^T)$.

(b) For the fixed phase velocity $c \in (c_1^T; c_2^T)$, there exist an infinite number of Love waves propagating with different frequencies ω.

Corollary 2. There do not exist Love waves if $c_1^T > c_2^T$.

In [9] it was shown that Love waves can propagate in the system consisting of an anisotropic layer and the half-space in contact with it. It was assumed that both the layer and the half-space possess an axis of elastic symmetry of the fourth or sixth orders oriented along the vector $\mathbf{m}$. For this system the propagation conditions and dispersion relations were similar to (1.4) and (1.5). In [10] based on the complex formalism dispersion relations for the Love waves in a transversally isotropic layer and a half-space were obtained.

For layered media consisting of a large number of layers contacting with the half-space there do not exist analytical solutions similar to (1.5). Dispersion relations for the Love wave in such media can be obtained numerically using two matrix methods initially proposed for analysis of Lamb waves. These methods are known as the transfer matrix method (sometimes this method is called the Thomson–Haskell method after the developers [11, 12]) and the global matrix method proposed in [13, 14]. The transfer matrix method is based on the successive solution of contact boundary value problems at interface boundaries and construction of corresponding transfer matrices. Below this method will be discussed in more detail. The global matrix method is based on the solution of ordinary differential equations with piecewise homogeneous coefficients resulting in the construction of the special "global" matrix.

After the appearance of the global matrix method, it was assumed that numerical realizations of this method result in more stable solutions than for the transfer matrix method. Then various modifications of these methods were proposed to make them numerically stable [15]. The problem of numerical stability becomes especially topical if the layered medium consists of a large number of layers. In this case the advantages of the transfer matrix method become more pronounced since the order of corresponding matrices does not change with the number of layers; in the case of the global matrix method the order of the corresponding matrix linearly increases with increasing number of layers.

Love waves in a single isotropic layer with a rough free surface on an isotropic half-space were studied in [16, 17]. In [14] the theoretical method for investigation of propagation of Love waves in a multilayered isotropic medium by reduction of the problem to the system of ordinary differential equations with piecewise constant coefficients was proposed.

In seismology Love waves are regularly registered in the case of seismic activity [18, 19] and underground explosions [20–22]. These waves are also used for identification of the properties of sedimentary [23–25] and nondestructive material defectoscopy [26]. It should be noted that, in most studies devoted to Love waves, it is assumed that the layer and the half-space are elastically isotropic or transversally isotropic. At the same time, for application of these waves in modern methods of nondestructive diagnostics, it is necessary to develop existing methods for account of elastic anisotropy of contacting materials.

1.2.2. Lamb waves. These waves first described in [27, 28] for an isotropic elastic layer with free boundary planes, unlike Love waves, as a rule consist of several partial waves with different polarization. Lamb waves are widely used in nondestructive methods of investigation due to their dispersion and insignificant attenuation. One of the first studies devoted to the application of Lamb waves for nondestructive diagnostics is monograph [29]; in this study detailed analysis of dispersion relations was performed, the structure of these waves was examined, and the existence of several branches in the spectrum of these waves was discovered. In [4] the correlation of Lamb waves with the so-called carrier wave propagating in membranes was studied.

According to [30], it is convenient to seek the field displacements in the Lamb wave in the form

$$\mathbf{u}(\mathbf{x}) = \sum_{k=1}^{6} Z_k \mathbf{u}_k(\mathbf{x}) = \sum_{k=1}^{6} Z_k \mathbf{m}_k e^{ir(\gamma_k \mathbf{v}\cdot\mathbf{x} + \mathbf{n}\cdot\mathbf{x} - ct)}, \quad (1.6)$$

where $\mathbf{u}$ are the field of displacements, $\mathbf{u}_k$ is the field of displacements caused by the kth partial wave, Z_k are the complex coefficients determined to a scalar factor from the boundary conditions, $\mathbf{m}_k$ in the general case are the normalized vector complex amplitudes determined using Christoffel equations, γ_k—Christoffel equations roots, r is the wave number, $\mathbf{v}$ is the vector of external unit normal to the median plane Π_v of the plate, $\mathbf{n} \in \Pi_v$ is the vector of the wave normal in the median plane which determines the direction of propagation of the wave front, and c is the phase velocity. For determination of the amplitudes $\mathbf{m}_k$, the Christoffel parameters γ_k, and the dispersion relations between the phase velocity and the wave number or frequency, usually the so-called Stroh formalism [31] or the generalized Hamiltonian formalism [30] are applied.

It is probable that the equations for description of propagation of Lamb waves in a multilayered plate with free boundary planes which consists of different contacting isotropic layers were first obtained in [12]. Later, this method, called the transformation matrix method, was also used for analysis of Lamb waves in layered plates with anisotropic layers. An alternative approach using the global matrix method designated for analysis of Lamb waves in layered plates was proposed in [14] and studied in detail in [32].

Here it should be noted that, although from the fundamental point of view both methods provide the study of waves in a medium containing any finite number of layers, practical difficulties connected with computer realization of these methods prevent from efficient study of waves in media containing more than five to seven different layers. This is related to the high sensitivity of these methods to rounding error. It can be shown that, generally speaking, the accuracy of calculation of dispersion dependences for Lamb and Love waves exponentially decreases with increasing number of layers.

One of the first publications on theoretical studies of propagation of Lamb waves in anisotropic layers was [33]. Later, similar methods were used for investigation of anisotropic plates in [34, 35], and in [36] a method was proposed that reduces the problem of the Lamb wave in a multilayered anisotropic plate to a sys-

tem of algebraic equations. In [26, 37, 38] an analytical equation for description of propagation of Lamb waves in a multilayered plate with anisotropic layers was obtained; however, simplifying hypotheses similar to Kirchhoff–Love hypotheses in the theory of plate bending were used.

In many cases the account of elastic symmetry of anisotropic layers makes it possible to simplify the analysis of Love waves, for example, in [14, 19, 39, 40] analytical expressions for the equation describing dispersion dependences of Lamb waves were obtained. In [15, 41] a numerical–analytical method was proposed for investigation of combined Lamb–Raleigh waves propagating in the system anisotropic layer–half-space. Studies of propagation of Lamb waves in media with arbitrary elastic anisotropy were begun not long ago [30].

In one of the first papers on investigation of Lamb waves in periodic layered composites [42], a six-dimensional complex formalism was applied; this formalism was earlier used only for analysis of Raleigh waves. In [43] transverse surface waves in a periodic layered plate were studied based on Floquet partial solutions. The heuristic method for analysis of Lamb waves in a periodic layered structure based on averaging was proposed in [44], and in [45] experimental verification of this averaging algorithm was performed. The result obtained in [45] is quite interesting: the resulting wave in the averaged medium represents the Raleigh wave, while in each layer it is the Lamb wave.

1.2.3. Raleigh waves. It was noted above that Raleigh waves propagate in an elastic half-space, attenuate in the depth, and have no dispersion. Nonetheless, these waves play an important role in nondestructive testing of multilayered systems, since, along with Lamb and Love waves, they occur in the half-space contacting with layers.

Starting with paper [46], in which basic equations describing the propagation of elastic surface waves in a homogeneous isotropic half-space were obtained, in all subsequent studies of surface waves it was assumed that such a wave consists of three partial waves,

$$\mathbf{u}(\mathbf{x}) = \sum_{k=1}^{3} Z_k \mathbf{u}_k(\mathbf{x}) = \sum_{k=1}^{3} Z_k \mathbf{m}_k e^{ir(\gamma_k \mathbf{v}\cdot\mathbf{x} + \mathbf{n}\cdot\mathbf{x} - ct)}; \quad (1.7)$$

here, the notation is the same as for Lamb waves (1.6). For existence of the Raleigh wave, it is necessary for all comprising surface waves to have the same wave number and the same phase velocity.

Remark 1.3. (a) Attenuation in the depth (for $\mathbf{v}\cdot\mathbf{x} < 0$) of the Raleigh wave can be achieved if all roots γ_k in representation (1.1) have a negative imaginary part, below which this condition is assumed to be satisfied;

(b) if the real part $\mathrm{Re}(\gamma_k)$ is nonzero, the corresponding wave is called the generalized Raleigh wave.

It should be noted that, while the polynomial equation for determination of the velocity of the surface wave propagating in an isotropic half-space was obtained by Raleigh [46], the analytical expression for the velocity determining it as a function of elastic parameters and density was obtained not long ago [47, 48]. Earlier approximate fractional linear formulas were used for this purpose [29, 49, 50].

Representation (1.7) was also used in [5, 51] for investigation of Raleigh waves propagating in planes with elastic symmetry in directions of crystallographic axes of cubic and tetragonal crystals. The following fundamental result was proved based on these studies: the nonexistence of forbidden directions coinciding with the directions of crystallographic axes in cubic, orthorhombic, and tetragonal crystals for Raleigh waves.

Numerical studies of propagation of Raleigh waves in crystals of different syngonies were performed in [52] based on the 3D complex formalism using representation (1.7). In the course of these studies, forbidden directions were not found, except for the cases in which the Raleigh wave degenerated into the transverse body wave.

In [53] the six-dimensional complex formalism was developed for description of displacement of linear dislocations in anisotropic media; later, this formalism was applied for analysis of propagation of surface waves in anisotropic media [54–60]. Corresponding analytical and numerical results proved the absence of forbidden directions for Raleigh waves of type (1.7). Note that in [55] and then [57] the following theorem on existence of Raleigh waves was proved: for any anisotropy of an elastic medium in any direction of propagation there exists either a true Raleigh wave attenuating for $\mathbf{v}\cdot\mathbf{x} < 0$ or the corresponding Raleigh wave degenerates into the transverse body wave. Thus, the problem of forbidden directions, seemingly, was unambiguously solved. Nonetheless, it was demonstrated in [59, 61, 62] that forbidden directions for canonical Raleigh waves of type (1.7) exist. Moreover, forbidden directions can coincide with the directions of crystallographic axes of cubic crystals. However, in these cases a wave of more complex structure attenuating in the depth [61] propagates instead of Raleigh wave (1.7). In conclusion it should be noted that, in the case of certain types of elastic anisotropy for canonical Raleigh waves, not only separate forbidden directions, but also forbidden planes, can exist [63]. Similar directions and planes can be found for canonical Lamb waves [30].

1.3. Experimental Studies

Acoustic measurements are especially important, since they can be used for direct measurement of mechanical properties of materials, and the application of high frequencies makes it possible to determine

the properties of thin films and microdefects. Usually in acoustic studies used for analysis of material properties, velocities, frequencies, and polarization of corresponding waves are registered. Then, using the comparison of obtained experimental data and theoretical models, it is possible to determine physical and mechanical properties of materials.

In microelectronics microheating of material by a point pulsed laser source is often used for acoustic studies; in the neighborhood of the heated spot, the material experiences practically instantaneous temperature jump. This heated spot serves as the center of dilatation and the source of acoustic waves. A linear pulsed Nd–YAG laser based on Q-transitions is often used for this purpose. This method provides creation of acoustic waves with quite a small length (~0.1–10 μm), which makes it possible to use these waves for analysis of the properties of thin film coatings with a thickness of up to 10 nm [9]. Depending on the element geometry, laser pulse duration, and hot spot size, both body and surface acoustic waves are generated, and the application of precision measurement devices (as a rule, Fabry–Perot of Michelson interferometers) provides separation of different types of acoustic waves by corresponding displacements at the free boundary [6–8, 64, 65]. In some cases, for filtering of undesirable waves, a system of comb filters is deposited on the surface for cutting-off undesirable modes of surface waves [66, 67].

Another method of generation of surface waves is action on the free surface of different sources of mechanical oscillations. In microelectronics piezo elements are especially often used for this purpose [5]. In the case of the half-space, this element is usually applied to simulate the Lamb problem concerning the action of a concentrated source applied to the boundary of the half-space.

1.4. Method Developed in this Study

In this study a modified transfer matrix method is developed; it is based on the application of hyperbolic functions in the representation for partial waves which is designated for analytical investigation of Love waves in anisotropic media with a small number of layers (1–3) and for numerical analysis of systems containing a large number of layers. It will be shown below that representation (1.1) turns out to be wrong if the Christoffel equation has multiple roots. The correct representation and corresponding modification of the transfer matrix method will be given below. The transfer matrix method will be used for obtaining resolving equations for SH waves with transverse horizontal polarization propagating in layered plates with free and fixed boundary surfaces. In this case, unlike Love waves, plates are not in contact with the half-space.

2. BASIC RELATIONS

Hereinafter, layers and the half-space are assumed homogeneous and linearly hyperelastic. The motion equations for the elastic homogeneous anisotropic medium can be written in the form

$$\mathbf{A}(\partial_x, \partial_t)\mathbf{u} \equiv \mathrm{div}_x \mathbf{C} \cdot\cdot \nabla_x \mathbf{u} - \rho \ddot{\mathbf{u}} = 0, \qquad (2.1)$$

where the four-valent elasticity tensor $\mathbf{C}$ is assumed to be positive definite,

$$\forall \mathbf{A} \quad (\mathbf{A} \cdot\cdot \mathbf{C} \cdot\cdot \mathbf{A}) \equiv \sum_{i,j,m,n} A_{ij} C^{ijmn} A_{mn} > 0.$$
$$\mathbf{A} \in \mathrm{sym}(R^3 \otimes R^3), \mathbf{A} \neq 0$$

Remark 2.1. (a) This remark is related to the symmetry of the elasticity tensor. It is assumed that all considered media possess planes of elastic symmetry coinciding with the sagittal plane $\mathbf{m} \cdot \mathbf{x} = 0$. This is equivalent to the fact that the elasticity tensor for all materials belongs to the monocline system. It can be shown [56] that the latter results in vanishing of all decomposable components of the elasticity tensor with an odd number of occurrences of the vector $\mathbf{m}$ (in orthogonal basis R^3 formed by the vector $\mathbf{m}$ and any orthogonal vectors belonging to the sagittal plane). In the case of monocline symmetry, the elasticity tensor contains 13 independent decomposable components.

(b) It will be shown below that monocline symmetry provides the sufficient condition for surface actions on any plane $\mathbf{v} \cdot \mathbf{x} = \mathrm{const}$ to be collinear to the vector $\mathbf{m}$.

Following [55, 56] we consider a more general than (1.1) representation for the Love wave,

$$\mathbf{m} f(irx') e^{ir(\mathbf{n} \cdot \mathbf{x} - ct)}, \qquad (2.2)$$

where $x' = \mathbf{v} \cdot \mathbf{x}$, similar to representation (1.1); f is the unknown scalar function; and r is the wave number. The exponential factor in the right-hand part of (2.2) corresponds to the propagation of the wave front in the direction $\mathbf{n}$ with the phase velocity c. Substituting representation (2.2) into Eq. (2.1) and taking into account **Remark 2.1**, we obtain the following differential equation:

$$\begin{aligned} &((\mathbf{m} \otimes \mathbf{v} \cdot\cdot \mathbf{C} \cdot\cdot \mathbf{v} \otimes \mathbf{m})\partial_{x'}^2 \\ &+ (\mathbf{m} \otimes \mathbf{v} \cdot \mathbf{C} \cdot \mathbf{n} \otimes \mathbf{m} + \mathbf{m} \otimes \mathbf{n} \cdot \mathbf{C} \cdot \mathbf{v} \otimes \mathbf{m})\partial_{x'} \\ &+ (\mathbf{m} \otimes \mathbf{n} \cdot\cdot \mathbf{C} \cdot\cdot \mathbf{n} \otimes \mathbf{m} - \rho c^2))f(irx') = 0. \end{aligned} \qquad (2.3)$$

The characteristic equation for (2.3) known as the Christoffel equation has the form

$$\begin{aligned} &(\mathbf{m} \otimes \mathbf{v} \cdot\cdot \mathbf{C} \cdot\cdot \mathbf{v} \otimes \mathbf{m})\gamma^2 \\ &+ (\mathbf{m} \otimes \mathbf{v} \cdot \mathbf{C} \cdot \mathbf{n} \otimes \mathbf{m} + \mathbf{m} \otimes \mathbf{n} \cdot \mathbf{C} \cdot \mathbf{v} \otimes \mathbf{m})\gamma \\ &+ (\mathbf{m} \otimes \mathbf{n} \cdot\cdot \mathbf{C} \cdot\cdot \mathbf{n} \otimes \mathbf{m} - \rho c^2) = 0. \end{aligned} \qquad (2.4)$$

The left-hand side of Eq. (2.4) represents the second-order polynomial with respect to the Christoffel parameter γ. Thus, for the studied elastic symmetry,

the Love wave in the layer can consist of two partial waves only.

3. DISPLACEMENTS AND SURFACE FORCES IN THE HALF-SPACE

Below it is assumed that the layered medium consists of n layers contacting with the half-space (unless the opposite is assumed), the lower index $n + 1$ being related to the half-space. Since the displacement field in the half-space should attenuate in the depth, the corresponding root of Eq. (2.4) should be complex with a negative imaginary part; see **Remark 1.1.**

The following proposition is satisfied.

Proposition 3.1. Attenuation in the depth in the monocline half-space is possible if and only if the phase velocity c belongs to the (nonempty) velocity interval

$$c \in \left(0; \sqrt{\rho_{n+1}^{-1}\left(\mathbf{m}\otimes\mathbf{n}\cdot\cdot\mathbf{C}_{n+1}\cdot\cdot\mathbf{n}\otimes\mathbf{m} - \frac{(\mathbf{m}\cdot\mathrm{sym}(\mathbf{n}\cdot\mathbf{C}_{n+1}\cdot\mathbf{v})\cdot\mathbf{m})^2}{(\mathbf{m}\otimes\mathbf{v}\cdot\cdot\mathbf{C}_{n+1}\cdot\cdot\mathbf{v}\otimes\mathbf{m})}\right)}\right), \tag{3.1}$$

where, for an arbitrary second rank tensor, $\mathbf{A}$: $\mathrm{sym}(\mathbf{A}) \equiv 1/2(\mathbf{A} + \mathbf{A}^t)$. For velocity interval (3.1), the corresponding Christoffel parameter γ_{n+1} is complex with a negative imaginary part,

$$\gamma_{n+1} = -\frac{\mathbf{m}\cdot\mathrm{sym}(\mathbf{n}\cdot\mathbf{C}_{n+1}\cdot\mathbf{v})\cdot\mathbf{m}}{\mathbf{m}\otimes\mathbf{v}\cdot\cdot\mathbf{C}_{n+1}\cdot\cdot\mathbf{v}\otimes\mathbf{m}} - i\sqrt{\frac{\mathbf{m}\otimes\mathbf{n}\cdot\cdot\mathbf{C}_{n+1}\cdot\cdot\mathbf{n}\otimes\mathbf{m} - \rho_{n+1}c^2}{\mathbf{m}\otimes\mathbf{v}\cdot\cdot\mathbf{C}_{n+1}\cdot\cdot\mathbf{v}\otimes\mathbf{m}} - \left(\frac{\mathbf{m}\cdot\mathrm{sym}(\mathbf{n}\cdot\mathbf{C}_{n+1}\cdot\mathbf{v})\cdot\mathbf{m}}{\mathbf{m}\otimes\mathbf{v}\cdot\cdot\mathbf{C}_{n+1}\cdot\cdot\mathbf{v}\otimes\mathbf{m}}\right)^2}. \tag{3.2}$$

Proof. Direct analysis of the roots of Eq. (2.4) shows that these roots are complex in the case of a negative discriminant, which yields the upper boundary in (3.1). Let us show that the radicand in (3.1) is positive. This follows from analysis of the quadratic polynomial

$$P(x) \equiv \mathbf{m}\otimes(x\mathbf{v}+\mathbf{n})\cdot\cdot\mathbf{C}_{n+1}\cdot\cdot(\mathbf{n}+x\mathbf{v})\otimes\mathbf{m}. \tag{3.3}$$

The right-hand side of (3.3) is positive for any real x, since the elasticity tensor is positive definite. The absence of real roots of this polynomial completes the proof, since the discriminant of this polynomial coincides (to the factor $-(\rho_{n+1})^{-1/2}$ with the upper boundary in (3.1)). It should be noted that expression (3.2) was obtained from the solution to Eq. (2.4).

Corollary 1. The parameter γ_{n+1} cannot be a multiple root of Christoffel equation (2.4).

The proof follows from the condition of nonvanishing discriminant of Eq. (3.2) which is necessary for attenuation of the wave in the depth.

Corollary 2. If the considered material possesses another plane of elastic symmetry the normal of which coincides with the vector $\mathbf{n}$ or $\mathbf{v}$ (such a material is necessarily orthotropic), the admissible velocity interval has the form

$$c \in (0; c_{n+1}^T),$$

where c_{n+1}^T is the velocity of the transverse body wave propagating in the direction of the vector $\mathbf{n}$ with the polarization coinciding with the vector $\mathbf{m}$. For the considered case, the Christoffel parameter γ_{n+1} is purely imaginary,

$$\gamma_{n+1} = -i\sqrt{\frac{\mathbf{m}\otimes\mathbf{n}\cdot\cdot\mathbf{C}_{n+1}\cdot\cdot\mathbf{n}\otimes\mathbf{m} - \rho_{n+1}c^2}{\mathbf{m}\otimes\mathbf{v}\cdot\cdot\mathbf{C}_{n+1}\cdot\cdot\mathbf{v}\otimes\mathbf{m}}}.$$

Proof. For such a material, the expression $(\mathrm{sym}(\mathbf{m}\otimes\mathbf{n}\cdot\cdot\mathbf{C}_{n+1}\cdot\cdot\mathbf{n}\otimes\mathbf{m}))$ in (3.2) vanishes, since this expression contains an odd number of occurrences of the vectors $\mathbf{n}$ and $\mathbf{v}$. It is sufficient to note that the remaining radicand in (3.1) coincides with the velocity c_{n+1}^T. The remaining part of the proof follows from the analysis of Eq. (2.4).

Representation (1.1) for the half-space yields the following field of surface forces on the plane $\mathbf{v}\cdot\mathbf{x} = 0$:

$$\mathbf{t}_{n+1}(\mathbf{x})|_{\mathbf{v}\cdot\mathbf{x}=0} = irC_{2n+1}(\gamma_{n+1}(\mathbf{v}\cdot\mathbf{C}_{n+1}\cdot\cdot\mathbf{v}\otimes\mathbf{m}) + (\mathbf{v}\cdot\mathbf{C}_{n+1}\cdot\cdot\mathbf{n}\otimes\mathbf{m}))e^{ir(\mathbf{n}\cdot\mathbf{x}-ct)}. \tag{3.4}$$

Proposition 3.2. Surface forces (3.4) are collinear to the vector $\mathbf{m}$.

The proof follows from the proposed monocline symmetry with respect to the vector $\mathbf{m}$, which provides an even number of occurrences of the vector $\mathbf{m}$ in the decomposable components of the tensor $\mathbf{C}_{n+1}$ in the basis formed by the vectors $\mathbf{m}$, $\mathbf{v}$, $\mathbf{n}$. Thus, the vectors $(\mathbf{v}\cdot\mathbf{C}_{n+1}\cdot\cdot\mathbf{v}\otimes\mathbf{m})$ and $(\mathbf{v}\cdot\mathbf{C}_{n+1}\cdot\cdot\mathbf{n}\otimes\mathbf{m})$ in the right-hand side of (3.4) are collinear to the vector $\mathbf{m}$.

4. DISPLACEMENTS AND SURFACE FORCES IN LAYERS

In this section the lower index k ($1 \le k \le n$) is related to the corresponding layer.

4.1. Nonmultiple Roots

For nonmultiple roots of Christoffel equations and the orthotropic material with the principal axes of elasticity coinciding with the vectors $\mathbf{m}$, $\mathbf{n}$, and $\mathbf{v}$, representation (1.1) is valid. However, in this analysis, which includes a more general class of monocline symmetry, representation (1.1) is modified as follows:

$$\mathbf{u}_k(\mathbf{x}) = \mathbf{m}(C_{2k-1}\sinh(ir\alpha_k x') + C_{2k}\cosh(ir\alpha_k x'))e^{ir(\beta_k x' + \mathbf{n}\cdot\mathbf{x} - ct)}, \tag{4.1}$$

where $\gamma_k = \alpha_k + \beta_k$.

$$\alpha_k = -i\sqrt{\frac{\mathbf{m}\otimes\mathbf{n}\cdot\cdot\mathbf{C}_k\cdot\cdot\mathbf{n}\otimes\mathbf{m} - \rho_k c^2}{\mathbf{m}\otimes\mathbf{v}\cdot\cdot\mathbf{C}_k\cdot\cdot\mathbf{v}\otimes\mathbf{m}} - \left(\frac{\mathbf{m}\cdot\mathrm{sym}(\mathbf{n}\cdot\mathbf{C}_k\cdot\mathbf{v})\cdot\mathbf{m}}{\mathbf{m}\otimes\mathbf{v}\cdot\cdot\mathbf{C}_k\cdot\cdot\mathbf{v}\otimes\mathbf{m}}\right)^2}, \qquad \beta_k = -\frac{\mathbf{m}\cdot\mathrm{sym}(\mathbf{n}\cdot\mathbf{C}_k\cdot\mathbf{v})\cdot\mathbf{m}}{\mathbf{m}\otimes\mathbf{v}\cdot\cdot\mathbf{C}_k\cdot\cdot\mathbf{v}\otimes\mathbf{m}}. \tag{4.2}$$

Thus, α_k is the real or imaginary parameter, depending on the value of the phase velocity, and β_k is real independently of the velocity c.

Taking into account (4.1), the corresponding surface forces on the plane $\mathbf{v}\cdot\mathbf{x} = x'$ have the form

$$\mathbf{t}_k(x') = ir\begin{pmatrix}\left((\mathbf{v}\cdot\mathbf{C}_k\cdot\cdot\mathbf{v}\otimes\mathbf{m})(\alpha_k\cosh(ir\alpha_k x') + \beta_k\sinh(ir\alpha_k x')) + (\mathbf{v}\cdot\mathbf{C}_k\cdot\cdot\mathbf{n}\otimes\mathbf{m})\sinh(ir\alpha_k x')\right)C_{2k-1} \\ +\left((\mathbf{v}\cdot\mathbf{C}_k\cdot\cdot\mathbf{v}\otimes\mathbf{m})(\alpha_k\sinh(ir\alpha_k x') + \beta_k\cosh(ir\alpha_k x')) + (\mathbf{v}\cdot\mathbf{C}_k\cdot\cdot\mathbf{n}\otimes\mathbf{m})\cosh(ir\alpha_k x')\right)C_{2k}\end{pmatrix} e^{ir(\beta_k x' + \mathbf{n}\cdot\mathbf{x} - ct)}. \tag{4.3}$$

Proposition 4.1. Surface forces (4.3) are collinear to the vector $\mathbf{m}$.

The proof is similar to the proof of **Proposition 3.2**.

Taking into account (4.3) and the fact that $\mathbf{v}\cdot\mathbf{C}_k\cdot\cdot\mathbf{n}\otimes\mathbf{m} = 0$, $\beta_k = 0$, and $\gamma_k = \alpha_k$, for the orthotropic material with axes of elastic symmetry coinciding with the vectors $\mathbf{m}$, $\mathbf{n}$, and $\mathbf{v}$, we obtain the following expression for the surface forces:

$$\mathbf{t}_k(x') = ir\gamma_k(\mathbf{v}\cdot\mathbf{C}_k\cdot\cdot\mathbf{v}\otimes\mathbf{m}) \times (C_{2k-1}\cosh(ir\gamma_k x') + C_{2k}\sinh(ir\gamma_k x'))e^{ir(\mathbf{n}\cdot\mathbf{x} - ct)}.$$

4.2. Multiple Roots

Representation (4.1) for Love waves in the layer is wrong if multiple roots occur in the Christoffel equation [10, 55]. Multiple roots occur if the parameter α_k in (4.2) vanishes; this yields the following proposition.

Proposition 4.2. (a) The phase velocity for which multiple roots occur is determined by the following expression:

$$c = \sqrt{\rho^{-1}\left(\mathbf{m}\otimes\mathbf{n}\cdot\cdot\mathbf{C}_k\cdot\cdot\mathbf{n}\otimes\mathbf{m} - \frac{(\mathbf{m}\cdot\mathrm{sym}(\mathbf{n}\cdot\mathbf{C}_k\cdot\mathbf{v})\cdot\mathbf{m})^2}{\mathbf{m}\otimes\mathbf{v}\cdot\cdot\mathbf{C}_k\cdot\cdot\mathbf{v}\otimes\mathbf{m}}\right)}. \tag{4.4}$$

(b) The corresponding Christoffel parameter γ_k (necessarily real) has the form

$$\gamma_k = -\frac{\mathbf{m}\cdot\mathrm{sym}(\mathbf{n}\cdot\mathbf{C}_k\cdot\mathbf{v})\cdot\mathbf{m}}{\mathbf{m}\otimes\mathbf{v}\cdot\cdot\mathbf{C}_k\cdot\cdot\mathbf{v}\otimes\mathbf{m}}. \tag{4.5}$$

(c) The representation of the field of displacements corresponding to multiple roots has the form

$$\mathbf{u}_k(\mathbf{x}) = \mathbf{m}(C_{2k-1} + irx'C_{2k})e^{ir(\gamma_k x' + \mathbf{n}\cdot\mathbf{x} - ct)}. \tag{4.6}$$

(d) The corresponding surface forces on the plane $\mathbf{v}\cdot\mathbf{x} = x'$ have the form

$$\mathbf{t}_k(x') = ir\begin{pmatrix}(\mathbf{v}\cdot\mathbf{C}_k\cdot\cdot\mathbf{v}\otimes\mathbf{m})(\gamma_k C_{2k-1} + (1+ir\gamma_k x')C_{2k})\\ +(\mathbf{v}\cdot\mathbf{C}_k\cdot\cdot\mathbf{n}\otimes\mathbf{m})(C_{2k-1} + irx'C_{2k})\end{pmatrix} e^{ir(\gamma_k x' + \mathbf{n}\cdot\mathbf{x} - ct)}. \quad (4.7)$$

Proof. Conditions (a) and (b) follow from the condition of vanishing of the discriminant in the right-hand side of (3.2). Condition (c) corresponds to the general solution to Eq. (2.3) in the case of multiple roots [10, 30, 62].

Proposition 4.3. Surface forces (4.7) are collinear to the vector $\mathbf{m}$.

The proof is similar to the proof of **Proposition 3.2.**

5. MODIFIED TRANSFER MATRIX METHOD

5.1. Transfer Matrices

According to **Propositions 4.1, 4.2**, the scalar amplitudes of displacements and surface forces in the kth layer on the plane $\mathbf{v}\cdot\mathbf{x} = x'$ can be represented in the form

$$\begin{pmatrix} u_k(x') \\ t_k(x')\end{pmatrix} = \mathbf{M}_k(x')\begin{pmatrix} C_{2k-1} \\ C_{2k}\end{pmatrix}, \quad (5.1)$$

where $u_k(x') \equiv \left|\mathbf{u}_k(x')e^{-ir(\mathbf{n}\cdot\mathbf{x}-ct)}\right|$, $t_k(x') \equiv \left|\mathbf{t}_k(x')e^{-ir(\mathbf{n}\cdot\mathbf{x}-ct)}\right|$ are the corresponding scalar amplitudes and $\mathbf{M}_k$ is the 2×2 matrix. Taking into account expressions (4.1), (4.3), (4.4), and (4.5), the matrix $\mathbf{M}_k$ takes the following form.

5.1.1. Nonmultiple roots

$$\mathbf{M}_k(x') = \left(\begin{array}{c|c} (ir)^{-1}\sinh(ir\alpha_k x') & (ir)^{-1}\cosh(ir\alpha_k x') \\ \hline \begin{pmatrix}(\mathbf{m}\otimes\mathbf{v}\cdot\cdot\mathbf{C}_k\cdot\cdot\mathbf{v}\otimes\mathbf{m})\begin{pmatrix}\alpha_k\cosh(ir\alpha_k x')\\ +\beta_k\sinh(ir\alpha_k x')\end{pmatrix}\\ +(\mathbf{m}\otimes\mathbf{v}\cdot\cdot\mathbf{C}_k\cdot\cdot\mathbf{n}\otimes\mathbf{m})\sinh(ir\alpha_k x')\end{pmatrix} & \begin{pmatrix}(\mathbf{m}\otimes\mathbf{v}\cdot\cdot\mathbf{C}_k\cdot\cdot\mathbf{v}\otimes\mathbf{m})\begin{pmatrix}\alpha_k\sinh(ir\alpha_k x')\\ +\beta_k\cosh(ir\alpha_k x')\end{pmatrix}\\ +(\mathbf{m}\otimes\mathbf{v}\cdot\cdot\mathbf{C}_k\cdot\cdot\mathbf{n}\otimes\mathbf{m})\cosh(ir\alpha_k x')\end{pmatrix}\end{array}\right) ire^{ir\beta_k x'}. \quad (5.2)$$

5.1.2. Multiple roots

$$\mathbf{M}_k(x') = \left(\begin{array}{c|c} (ir)^{-1} & x' \\ \hline \begin{pmatrix}\gamma_k(\mathbf{m}\otimes\mathbf{v}\cdot\cdot\mathbf{C}_k\cdot\cdot\mathbf{v}\otimes\mathbf{m})\\ +(\mathbf{m}\otimes\mathbf{v}\cdot\cdot\mathbf{n}\otimes\mathbf{m})\end{pmatrix} & \begin{pmatrix}(1+ir\gamma_k x')(\mathbf{m}\otimes\mathbf{v}\cdot\cdot\mathbf{C}_k\cdot\cdot\mathbf{v}\otimes\mathbf{m})\\ +irx'(\mathbf{m}\otimes\mathbf{v}\cdot\cdot\mathbf{C}_k\cdot\cdot\mathbf{n}\otimes\mathbf{m})\end{pmatrix}\end{array}\right) ire^{ir\gamma_k x'}. \quad (5.3)$$

Note that according to (4.2) the parameter β_k in (5.2) is independent of the phase velocity c. The following proposition is satisfied.

Proposition 5.1. Independently of multiplicity of roots the matrices $\mathbf{M}_k$ are nondegenerate for any real x'.

Proof. Note that the exponential factors $e^{ir\beta_k x'}$ in (5.2) and $e^{ir\gamma_k x'}$ in (5.3) are nonzero for any x'. Direct analysis shows that the matrices in the right-hand sides of (5.2), (5.3) are nondegenerate for any x', the determinant of the matrix in (5.2) is $-\alpha_k(\mathbf{m}\otimes\mathbf{n}\cdot\cdot\mathbf{C}_k\cdot\cdot\mathbf{n}\otimes\mathbf{m})e^{ir\beta_k x'}$ and $\alpha_k \neq 0$, since the roots are nonmultiple. In the case of matrix (5.3) the corresponding determinant is $(\mathbf{m}\otimes\mathbf{v}\cdot\cdot\mathbf{C}_k\cdot\cdot\mathbf{v}\otimes\mathbf{m})e^{ir\gamma_k x'}$.

Then using the matrices $\mathbf{M}_k$, the displacements, and the surface forces at the interface between the nth layer and the half-space can be represented in terms of the coefficients C_1 and C_2 only,

$$\begin{pmatrix} u_n(-h_n/2) \\ t_n(-h_n/2)\end{pmatrix} = \left(\prod_{k=2}^{n}(\mathbf{M}_k(-h_k/2)\cdot\mathbf{M}_k^{-1}(h_k/2))\right)\cdot\mathbf{M}_1(-h_1/2)\begin{pmatrix} C_1 \\ C_2\end{pmatrix}, \quad (5.4)$$

where h_k, $k = 1, ..., n$ are the thicknesses of the corresponding layers.

5.2. Boundary Conditions at the External Boundary

Expressions (4.3), (4.7) yield the conditions of absence of tangent stresses at the external boundary for the first layer,

$$t_1(h_1/2) \equiv \vec{B}_1(h_1/2) \cdot \vec{C} = 0,$$

where t_1 is corresponding scalar amplitude; $\vec{B}_1(h_1/2) = (X_1(h_1/2); Y_1(h_1/2))$, and $\vec{C} = (C_1; C_2)$. The components $X_1(h_1/2)$ and $Y_1(h_1/2)$ have the following form.

5.2.1. Nonmultiple roots

$$X_1(h_1/2) = \left((\mathbf{m}\otimes\mathbf{v}\cdot\cdot\mathbf{C}_1\cdot\cdot\mathbf{v}\otimes\mathbf{m})(\alpha_1\cosh(ir\alpha_1h_1/2)+\beta_1\sinh(ir\alpha_1h_1/2)) + (\mathbf{m}\otimes\mathbf{v}\cdot\cdot\mathbf{C}_1\cdot\cdot\mathbf{n}\otimes\mathbf{m})\sinh(ir\alpha_1h_1/2)\right) ire^{ir\beta_1h_1/2},$$
$$Y_1(h_1/2) = \left((\mathbf{m}\otimes\mathbf{v}\cdot\cdot\mathbf{C}_1\cdot\cdot\mathbf{v}\otimes\mathbf{m})(\alpha_1\sinh(ir\alpha_1h_1/2)+\beta_1\cosh(ir\alpha_1h_1/2)) + (\mathbf{m}\otimes\mathbf{v}\cdot\cdot\mathbf{C}_1\cdot\cdot\mathbf{n}\otimes\mathbf{m})\cosh(ir\alpha_1h_1/2)\right) ire^{ir\beta_1h_1/2}. \quad (5.5)$$

5.2.2. Multiple roots

$$X_1(h_1/2) = (\gamma_1(\mathbf{m}\otimes\mathbf{v}\cdot\cdot\mathbf{C}_1\cdot\cdot\mathbf{v}\otimes\mathbf{m}) + (\mathbf{m}\otimes\mathbf{v}\cdot\cdot\mathbf{C}_1\cdot\cdot\mathbf{n}\otimes\mathbf{m}))ire^{ir\gamma_1h_1/2},$$
$$Y_1(h_1/2) = ((1+ir\gamma_1h_1/2)(\mathbf{m}\otimes\mathbf{v}\cdot\cdot\mathbf{C}_1\cdot\cdot\mathbf{v}\otimes\mathbf{m}) + irh_1/2(\mathbf{m}\otimes\mathbf{v}\cdot\cdot\mathbf{C}_1\cdot\cdot\mathbf{n}\otimes\mathbf{m}))ire^{ir\gamma_1h_1/2}. \quad (5.6)$$

Equations (5.1) make it possible to express (to a factor) the coefficients C_1 and C_2 in the form of solution to the following equation:

$$\vec{T}_1(h_1/2) \times \vec{C} = 0, \quad (5.7)$$

where

$$\vec{T}_1(h_1/2) = (-Y_1(h_1/2); X_1(h_1/2)). \quad (5.8)$$

It can be seen from (5.7) that the two-dimensional vector $\vec{T}_1(h_1/2)$ is collinear to the vector $\vec{C}$.

5.3. Boundary Conditions at the Interface nth Layer–Half-space

The contact conditions at the corresponding interface can be represented in the form

$$\vec{V}_n(-h_n/2) \times \vec{W}_{n+1}(0) = 0, \quad (5.9)$$

where

$$\vec{V}_n(-h_n/2) = (u_n(-h_n/2), t_n(-h_n/2)), \quad (5.10)$$

$$\vec{W}_{n+1}(0) = (-t_{n+1}(0), u_{n+1}(0)). \quad (5.11)$$

In (5.11) $t_{n+1}(0) = \left|\mathbf{t}_{n+1}(0)e^{-ir(\mathbf{n}\cdot\mathbf{x}-ct)}\right|$, and the vector $\mathbf{t}_{n+1}(0)$ is determined according to (3.4). Taking into account (5.10), (5.11), it can be seen that Eq. (5.9) expresses the collinearity of the vectors $\vec{V}_n$ and $(u_{n+1}(0), t_{n+1}(0))$, which is equivalent to the condition of collinearity of displacements and forces upon passing over the interface of components. In (5.11) it is assumed that, in the local coordinate system for the half-space, the interface plane is determined by the equation $\mathbf{v}\cdot\mathbf{x} = 0$.

5.4. Resolving Equation for Love Waves

Taking into account Eqs. (5.4), (5.7), (5.9), and (5.11), the united equation of modified transfer matrix method can be represented in the form

$$\vec{W}_{n+1}(0) \cdot \left(\left(\prod_{k=2}^{n} \mathbf{M}_k(-h_k/2)\cdot\mathbf{M}_k^{-1}(h_k/2)\right) \times \mathbf{M}_1(-h_1/2)\right) \cdot \vec{T}_1(h_1/2) = 0. \quad (5.12)$$

Equation (5.12) represents the sought resolving equation for Love waves.

5.5. Resolving Equation for Horizontally Polarized Shear Waves in Layered Plates

In this section the resolving equation for the horizontally polarized shear waves propagating in the layered plate consisting of n layers ($n > 1$) will be obtained. The external surfaces of the plate are assumed to be free from surface forces, or fixed, or possess mixed boundary conditions (one of the surfaces is free from forces, and the other one is fixed).

5.5.1. Layered plate with free external boundary plates. For such a plate, the corresponding boundary conditions have the form

$$\begin{cases} \mathbf{t}_1(h_1/2) \equiv \nu \cdot \mathbf{C}_1 \cdot \nabla \mathbf{u} = 0, \\ \mathbf{t}_n(-h_n/2) \equiv \nu \cdot \mathbf{C}_n \cdot \nabla \mathbf{u} = 0. \end{cases} \tag{5.13}$$

Similarly to Section 5.4, the application of the modified transfer matrix method provides the resolving equation in the form

$$\vec{T}_n(-h_n/2) \times \mathbf{M}_n^{-1}(h_n/2) \times \left(\prod_{k=2}^{n-1} \mathbf{M}_k(-h_n/2) \times \mathbf{M}_k^{-1}(h_k/2) \right) \times \mathbf{M}_1(-h_1/2) \times \vec{T}_1(h_1/2) = 0, \tag{5.14}$$

where the 2D vectors $\vec{T}_1$ and $\vec{T}_n$ corresponding to boundary conditions (5.13) have the form

$$\begin{aligned} \vec{T}_1(h_1/2) &= (-Y_1(h_1/2); X_1(h_1/2)), \\ \vec{T}_n(-h_n/2) &= (X_n(-h_n/2); Y_n(-h_n/2)). \end{aligned} \tag{5.15}$$

In (5.15) the components X_k, Y_k, $K = 1, n$, are determined using (5.5), (5.6).

5.5.2. Layered plate with fixed boundary surfaces. For such a plate, the boundary conditions have the form

$$\begin{cases} \mathbf{u}_1(h_1/2) = 0, \\ \mathbf{u}_n(-h_n/2) = 0. \end{cases}$$

The application of the modified transfer matrix method yields the following resolving equation:

$$\vec{D}_n(-h_n/2) \times \mathbf{M}_n^{-1}(h_n/2) \times \left(\prod_{k=2}^{n-1} \mathbf{M}_k(-h_n/2) \times \mathbf{M}_k^{-1}(h_k/2) \right) \times \mathbf{M}_1(-h_1/2) \times \vec{D}_1(h_1/2) = 0, \tag{5.16}$$

where the vectors $\vec{D}_1(h_1/2)$, $\vec{D}_n(-h_n/2)$ can be represented in the form

$$\begin{aligned} \vec{D}_1(h_1/2) &= (-U_1(h_1/2); S_1(h_1/2)), \\ \vec{D}_n(-h_n/2) &= (S_n(-h_1/2); U_n(-h_n/2)). \end{aligned} \tag{5.17}$$

In (5.17) the components S_k, U_k, $k = 1, n$, for the case of nonmultiple roots, according to (4.1), have the form

$$S_k(\pm h_k/2) = \pm \sinh(ir\alpha_k h_k/2),$$

$$U_k(\pm h_k/2) = \cosh(ir\alpha_k h_k/2),$$

where the parameter α_k is determined by (4.2).

The components S_k, U_k, $k = 1, n$, for the case of *multiple* roots, according to (4.6), have the form

$$S_k(\pm h_k/2) = 1,$$

$$U_k(\pm h_k/2) = \pm irh_k/2.$$

5.5.3. Layered plate with one fixed and one free surface. For such a plate, the boundary conditions have the form

$$\begin{cases} \mathbf{t}(h_1/2) = 0, \\ \mathbf{u}_n(-h_n/2) = 0. \end{cases} \tag{5.18}$$

In (5.18) it is assumed that the upper boundary plane is free and the lower is fixed. For these boundary conditions, the resolving equation has the form

$$\vec{D}_n(-h_n/2) \times \mathbf{M}_n^{-1}(h_n/2) \times \left(\prod_{k=2}^{n-1} \mathbf{M}_k(-h_n/2) \times \mathbf{M}_k^{-1}(h_k/2) \right) \times \mathbf{M}_1(-h_1/2) \times \vec{T}_1(h_1/2) = 0. \tag{5.19}$$

The modification of Eq. (5.19) for the case in which the upper surface is fixed and the lower is free is obvious.

Remark 5.1. The left-hand sides of Eqs. (5.12), (5.14), (5.16), and (5.19) can be considered as implicit equations with respect to the wave number r for fixed phase frequency ω and vice versa. Using the relation

$$r = \frac{\omega}{c}$$

in these equations, the dispersion equation expressing the dependence of the phase frequency on the phase velocity can be obtained (generally speaking, this equation is implicit).

6. SOME ANALYTICAL SOLUTIONS

6.1. One Orthotropic Layer on an Orthotropic Half-Space

Let the vectors $\mathbf{v}$, $\mathbf{n}$, and $\mathbf{m}$ coincide with the principal axes of elasticity of the layer and the half-space. In this case the Christoffel parameters γ_k take the form

$$\gamma_k = (-1)^{k+1} i \sqrt{\frac{\mathbf{m} \otimes \mathbf{n} \cdot \cdot \mathbf{C}_k \cdot \cdot \mathbf{n} \otimes \mathbf{m} - \rho_k c^2}{\mathbf{m} \otimes \mathbf{v} \cdot \cdot \mathbf{C}_k \cdot \cdot \mathbf{v} \otimes \mathbf{m}}}, \quad k = 1, 2. \tag{6.1}$$

In (6.1) and below in this section, the index 1 denotes the layer and the index 2 denotes the half-space.

Remark 6.1. (a) Expression (6.1) shows that multiple roots for the characteristic equation in the layer can occur only if the phase velocity coincides with the velocity of the transverse body wave polarized in the direction of the vector $\mathbf{m}$ propagating in the direction $\mathbf{n}$.

(b) In spite of the fact that some analytical results for the orthotropic layer on the orthotropic half-space

were obtained in [5], the corresponding explicit dispersion equation was not obtained.

The scalar amplitude of surface forces $t_1(x') \equiv \left|\mathbf{t}_1(x')e^{-ir(\mathbf{n}\cdot\mathbf{x}-ct)}\right|$ on the plane $\mathbf{v}\cdot\mathbf{x} = x'$ in the layer has the following form.

6.1.1. Nonmultiple roots

$$t_1(x') = ir\gamma_1(\mathbf{m}\otimes\mathbf{v}\cdot\cdot\mathbf{C}_1\cdot\cdot\mathbf{v}\otimes\mathbf{m}) \times (C_1\cosh(ir\gamma_1 x') + C_2\sinh(ir\gamma_1 x')). \quad (6.2)$$

6.1.2. Multiple roots ($\gamma_1 = 0$)

$$t_1 = ir(\mathbf{m}\otimes\mathbf{v}\cdot\cdot\mathbf{C}_1\cdot\cdot\mathbf{v}\otimes\mathbf{m})C_2. \quad (6.3)$$

The scalar amplitude of surface forces $t_2(0) = \left|\mathbf{t}_2(0)e^{-ir(\mathbf{n}\cdot\mathbf{x}-ct)}\right|$ on the plane $\mathbf{v}\cdot\mathbf{x} = 0$ in the half-space has the form

$$t_2(0)|_{\mathbf{v}\cdot\mathbf{x}=0} = ir\gamma_2 x(\mathbf{m}\otimes\mathbf{v}\cdot\cdot\mathbf{C}_2\cdot\cdot\mathbf{v}\otimes\mathbf{m})C_3. \quad (6.4)$$

Proposition 6.1. There do not exist Love waves propagating in an orthotropic layer on an orthotropic half-space if the Christoffel equation for the layer has multiple roots.

Proof. Expressions (4.4) and (6.1) show that the multiple root γ_1 is necessarily zero. In this case condition of absence of surface forces (5.6) and (5.7) together with expression (6.3) yields

$$C_2 = 0. \quad (6.5)$$

Interface conditions (5.9) together with (6.3)–(6.5) provide

$$C_3 = 0. \quad (6.6)$$

Condition (6.6) provides the absence of displacements on the interface plane and results in the following:

$$C_1 = 0. \quad (6.7)$$

Conditions (6.5)–(6.7) complete the proof.

Eliminating multiple roots we consider the case of nonmultiple roots. The application of (5.2) to the orthotropic layer yields

$$\mathbf{M}_1(x') = \left(\begin{array}{c|c} \sinh(ir\gamma_1 x') & \cosh(ir\gamma_1 x') \\ \hline ir\gamma_1(\mathbf{m}\otimes\mathbf{v}\cdot\cdot\mathbf{C}_1\cdot\cdot\mathbf{v}\otimes\mathbf{m})\cosh(ir\gamma_1 x) & ir\gamma_1(\mathbf{m}\otimes\mathbf{v}\cdot\cdot\mathbf{C}_1\cdot\cdot\mathbf{v}\otimes\mathbf{m})\sinh(ir\gamma_1 x') \end{array}\right). \quad (6.8)$$

The vector $\vec{T}_1$ determined using (5.8) to the scalar factor $ir\gamma_1(\mathbf{m}\cdot\mathbf{v}\cdot\cdot\mathbf{C}_1\cdot\cdot\mathbf{v}\otimes\mathbf{m})$ can be represented in the form

$$\vec{T}_1(h_1/2) = (-\sinh(ir\gamma_1 h_1/2); \cosh(ir\gamma_1 h_1/2)). \quad (6.9)$$

Similarly, the vector $\vec{W}_2$ determined using (5.11) has the form

$$\vec{W}_2 = (-ir\gamma_2\mathbf{m}\otimes\mathbf{v}\cdot\cdot\mathbf{C}_2\cdot\cdot\mathbf{v}\otimes\mathbf{m}; 1). \quad (6.10)$$

Substituting (6.8)–(6.10) into Eq. (5.12) after some transformations yields

$$\omega = \frac{c}{\gamma_1 h_1}\left(\arctan\left(i\frac{\zeta_2}{\zeta_1}\right) + n\pi\right), \quad n = 0, 1, 2, \ldots, \quad (6.11)$$

where $\zeta_k = \gamma_k(\mathbf{m}\otimes\mathbf{v}\cdot\cdot\mathbf{C}_k\cdot\cdot\mathbf{v}\otimes\mathbf{m})$, $k = 1, 2$.

Proposition 6.2. (a) In the considered case Love waves can propagate only if the phase velocity belongs to the interval $c \in (c_1^T; c_2^T)$ (for this velocity interval all roots of Christoffel equation are nonmultiple), where

$$c_k^T = \sqrt{\frac{\mathbf{m}\otimes\mathbf{n}\cdot\cdot\mathbf{C}_k\cdot\cdot\mathbf{n}\otimes\mathbf{m}}{\rho_k}}, \quad k = 1, 2,$$

are the velocities of the corresponding shear body waves with the polarization vector $\mathbf{m}$.

(b) For the fixed frequency ω, there exist not more than a finite number of Love waves propagating with different phase velocities $c \in (c_1^T; c_2^T)$.

(c) For fixed velocity $c \in (c_1^T; c_2^T)$, there exists a countable set of Love waves propagating with different frequencies ω.

Proof. (a) Let us assume that $c_1^T < c_2^T$; then the corresponding velocity range is nonempty. Analysis of expression (6.11) shows that, for the phase velocity in the interval $(c_1^T; c_2^T)$, the Christoffel parameter γ_1 determined using (6.1) is real and negative, while γ_2 determined using (6.2) is imaginary with a negative imaginary part. Substituting γ_k, $k = 1, 2$ into (6.11) we obtain the positive values of the phase velocity ω. Assuming that $c < c_1^T$, we obtain

$$\omega = -\frac{c}{|\gamma_1| h_1}\tanh^{-1}\left(\left|\frac{\zeta_2}{\zeta_1}\right|\right). \quad (6.11')$$

It follows from (6.11') that, in this velocity range, the right-hand side of frequency (6.11') is negative, which is impossible. The other statements directly follow from (6.11).

Corollary. In the considered case there do not exist Love waves if $c_1^T > c_2^T$.

6.2. Two Orthotropic Layers on Orthotropic Half-Space (Nonmultiple Roots)

Using the notation introduced above, we obtain the following expression for the product of transfer matrices:

$$\mathbf{M}_2(-h_2/2)\cdot\mathbf{M}_2^{-1}(h_2/2)\cdot\mathbf{M}_1(-h_1/2) = \begin{pmatrix} a_{11} & a_{12} \\ a_{21} & a_{22} \end{pmatrix}, \tag{6.12}$$

where

$$\begin{aligned} a_{11} &= -i\left(\cos(\xi_2)\sin\left(\frac{1}{2}\xi_1\right) + \frac{\zeta_1}{\zeta_2}\sin(\xi_2)\cos\left(\frac{1}{2}\xi_1\right)\right), \\ a_{12} &= \cos(\xi_2)\cos\left(\frac{1}{2}\xi_1\right) - \frac{\zeta_1}{\zeta_2}\sin(\xi_2)\sin\left(\frac{1}{2}\xi_1\right), \\ a_{21} &= -ir\zeta_2\left(\sin(\xi_2)\sin\left(\frac{1}{2}\xi_1\right) - \frac{\zeta_1}{\zeta_2}\cos(\xi_2)\cos\left(\frac{1}{2}\xi_1\right)\right), \\ a_{22} &= r\zeta_2\left(\sin(\xi_2)\cos\left(\frac{1}{2}\xi_2\right) + \frac{\zeta_1}{\zeta_2}\cos(\xi_2)\sin\left(\frac{1}{2}\xi_1\right)\right), \\ \xi_k &= r\gamma_k h_k, \\ \zeta_k &= \gamma_k(\mathbf{m}\otimes\mathbf{v}\cdot\cdot\,\mathbf{C}_k\cdot\cdot\,\mathbf{v}\otimes\mathbf{m}),\quad k = 1, 2, 3. \end{aligned} \tag{6.13}$$

In (6.13) the indices 1 and 2 denote the layers and the index 3 denotes the half-space.

Expressions (6.9) and (6.10) for the vectors $\vec{T}_1$ and $\vec{W}_3$ are the same but with obvious change of indices. Substituting (6.12), (6.13) into Eq. (5.12) yields the resolving equation in the form

$$\sin\xi_2\left(\cos\xi_1 + i\frac{\zeta_3\zeta_1}{\zeta_2^2}\sin\xi_1\right) - \cos\xi_2\left(i\frac{\zeta_3}{\zeta_2}\cos\xi_1 - \frac{\zeta_1}{\zeta_2}\sin\xi_1\right) = 0. \tag{6.14}$$

Unlike the previous case, Eq. (6.14), generally speaking, cannot be resolved with respect to the phase frequency ω.

6.3. Two Orthotropic Half-Spaces with an Orthotropic Layer between Them

Taking into account **Corollary 1** of **Proposition 3.1**, the case resulting in multiple roots for half-spaces should be eliminated from consideration. At the same time, according to **Remark 6.1** (a) multiple roots in Christoffel equation for the orthotropic layer occur only if the phase velocity coincides with the velocity of the transverse body wave and the corresponding Christoffel parameter γ_2 becomes zero. Then using arguments similar to those used for proving **Proposition 6.1** we obtain the following statement.

Proposition 6.3. There do not exist Love waves in the system formed by two orthotropic half-spaces and the orthotropic layer between them if a multiple root in Christoffel equation for the layer occurs.

Eliminating multiple roots we consider the case of *nonmultiple* roots in the Christoffel equation for the layer. The assumption that in both half-spaces the wave attenuates in the depth results in seeking the solution for phase velocities satisfying the inequality

$$c < \min(c_1^T; c_3^T), \tag{6.15}$$

where c_1^T, c_3^T denote the velocities of horizontally polarized transverse body waves propagating in the corresponding half-spaces in the direction of the vector **n**. Condition (6.15) provides nonzero imaginary parts of the Christoffel parameters γ_1, γ_3.

Remark 6.2. Attenuation in the depth in the "upper" half-space ($x' \to +\infty$) is provided by the choice of γ_1 with a positive imaginary part.

Transferring to the limit $h_1 \to \infty$ in Eq. (6.14) and taking into account **Remark 6.2**, we obtain the sought dispersion relation in the form

$$\omega = \frac{c}{\gamma_2 h_2}\left(\arctan\left(i\frac{\zeta_2(\zeta_3-\zeta_1)}{\zeta_2^2-\zeta_1\zeta_3}\right) + n\pi\right), \quad n = m, m+1, m+2, \ldots. \tag{6.16}$$

The parameter m in the right-hand side of (6.16) provides positiveness of the frequencies ω. Below this parameter will be determined explicitly. Obviously for $\zeta_1 = 0$ (vacuum) dispersion relation (6.16) is transformed into relation (6.11).

Proposition 6.4. (a) In the considered system, the Love wave can propagate only if the phase velocity belongs to the interval

$$c \in (c_2^T; \min(c_1^T, c_3^T)). \tag{6.17}$$

(b) For the fixed frequency ω there exist not more than a finite number of Love waves propagating with different velocities from interval (6.17).

(c) For the fixed phase velocity from interval (6.17) (under the condition that this interval is nonempty) there exists a countable number of Love waves propagating with different frequencies ω.

Proof. (a) If $c > \min(c_1^T, c_3^T)$, the Love wave cannot propagate since the attenuation condition in the half-spaces is not satisfied. Let us assume that $c < \min(c_1^T; c_2^T; c_3^T)$, then all parameters γ_k turn out to be imaginary,

$$\gamma_1 = +i|\gamma_1|, \quad \gamma_2 = \pm i|\gamma_2|, \quad \gamma_3 = -i|\gamma_3|. \tag{6.18}$$

Remark 6.2 was taken into account for choosing the signs in (6.18). Substituting (6.18) into (6.16) yields

$$\omega = -\frac{c}{|\gamma_2|h_2}\tanh^{-1}\left(\frac{|\zeta_2|(|\zeta_3|+|\zeta_1|)}{|\zeta_2|^2+|\zeta_1||\zeta_3|}\right). \quad (6.19)$$

In this case the right-hand side of (6.19) is negative, which is impossible.

Then let us show that, for the phase velocity from interval (6.17), the corresponding frequency ω is positive. For this velocity interval, we have

$$\gamma_1 = +i|\gamma_1|, \quad \gamma_2 = \pm|\gamma_2|, \quad \gamma_3 = -i|\gamma_3|. \quad (6.20)$$

Substituting (6.20) into (6.16) we obtain

$$\omega = \frac{c}{|\gamma_2|h_2}\left(\arctan\left(\frac{|\zeta_2|(|\zeta_3|+|\zeta_1|)}{|\zeta_2|^2-|\zeta_1||\zeta_3|}\right)+n\pi\right), \quad (6.16')$$

$$n = m, m+1, m+2, \ldots,$$

where the integer parameter m in the right-hand side of (6.16') is determined from the condition

$$m = -\mathrm{Ent}\left(\pi^{-1}\arctan\left(\frac{|\zeta_2|(|\zeta_3|+|\zeta_1|)}{|\zeta_2|^2-|\zeta_1||\zeta_3|}\right)\right). \quad (6.21)$$

Condition (6.21) provides positiveness of ω, where Ent(...) denotes the integer part.

The proof of propositions (b) and (c) follows from (6.16').

Corollary. The Love wave cannot propagate if $c_2^T > \min(c_1^T, c_3^T)$.

Remark 6.3. The results obtained in this section can serve as the explanation of occurrence of the high frequency waveguide for waves with transverse horizontal polarization propagating in the system consisting of the orthotropic layer between the orthotropic half-spaces.

7. NUMERICAL RESULTS

7.1. Love Waves in Multilayered Media

7.1.1. Love waves in ten-layered medium. For analysis of propagation of waves in media containing a large number of layers, a numerical algorithm based on the modified transfer matrix method was developed; it uses high-precision arithmetics (mantissa > 60 decimal digits). This allowed an investigation of propagation of Love waves in the medium consisting of ten alternating elastically isotropic SiC and Si_3N_4 nanolayers with a thickness of 10 nm each, which are at rest on the transversally isotropic silicon monocrystal.

Below we present the physical and mechanical properties of studied materials necessary for calculations,

(a) silicon monocrystal (Si), orientation 100,

$$C^{1212} = 79.913 \text{ GPa}, \quad \rho = 2339.9 \text{ kg/m}^3; \quad (7.1)$$

(b) silicon carbide (SiC),

$$C^{1212} = 122.80 \text{ GPa}, \quad \rho = 3100 \text{ kg/m}^3; \quad (7.2)$$

(c) silicon nitride (Si_3N_4),

$$C^{1212} = 61.447 \text{ GPa}, \quad \rho = 3290 \text{ kg/m}^3. \quad (7.3)$$

The parameter values correspond to a temperature of 20°C.

Figure 1 shows the dispersion curves for the considered multilayered material.

Figure 2 shows the plots characterizing the change of the lower dispersion branch Δ (as the most convenient in experimental studies) with increasing thickness of the kth layer by 10% (the other layer parameters remain unchanged),

$$\Delta = D_0^{k+10\%h} - D_0^{\mathrm{ref}}. \quad (7.4)$$

In (7.4) D_0^{ref} is the lower branch of the dispersion curves for the original configuration and $D_0^{k+10\%h}$ is the same branch with the thickness of the kth layer increased by 10%; in this case the layer enumeration begins with the upper layer.

Figure 3 shows similar dependences constructed for the shear modulus and density of the kth layer increased by 10% (simultaneous proportional change of these characteristics does not change the velocity of the corresponding transverse body wave).

The dependences shown in Figs. 2 and 3 show that the lower branch of the dispersion curves is informative and demonstrates the change of geometry of any of the deep layers and the change of their physical and chemical properties.

7.1.2. Love Waves in Two-Layered Composite. The study of a two-layered composite containing two layers with a thickness of 10 and 1 nm, respectively, in contact with the transversally isotropic half-space was more difficult from the technical point of view. The half-space and the layers possessed physical and mechanical characteristics determined by expressions (7.1)–(7.3).

Figure 4 shows the corresponding dispersion curves for the considered composite. It should be noted that the constructed dependences in the range above 4–5 THz are mainly of academic interest, since, as was

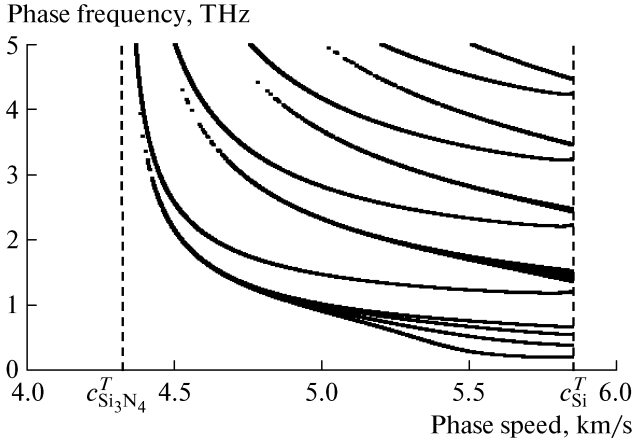

Fig. 1. Dispersion curves for Love waves propagating in the ten-layered plate in contact with the half-space.

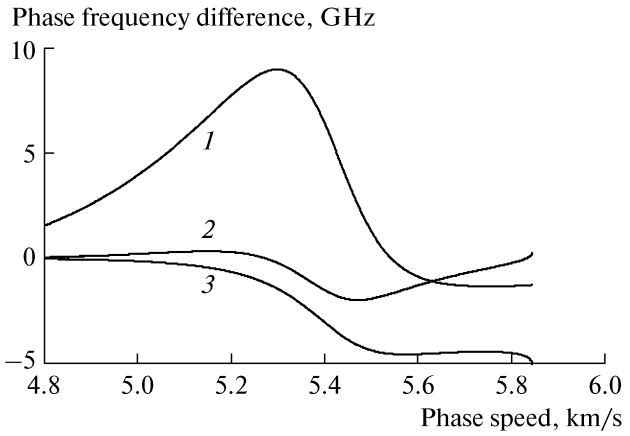

Fig. 2. Change of lower branch of dispersion curve for 10% variation of thickness of the (*1*) seventh, (*2*) ninth, and (*3*) tenth layers.

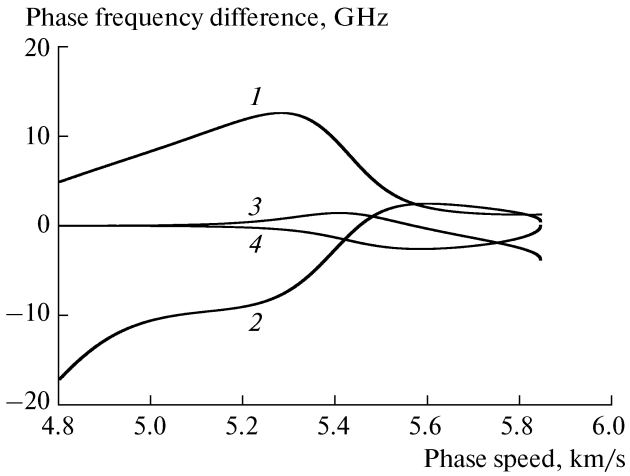

Fig. 3. Change of lower branch of dispersion curve for 10% variation of the shear modulus and density of the (*1*) seventh, (*2*) ninth, and (*3*) tenth layers and (*4*) the half-space.

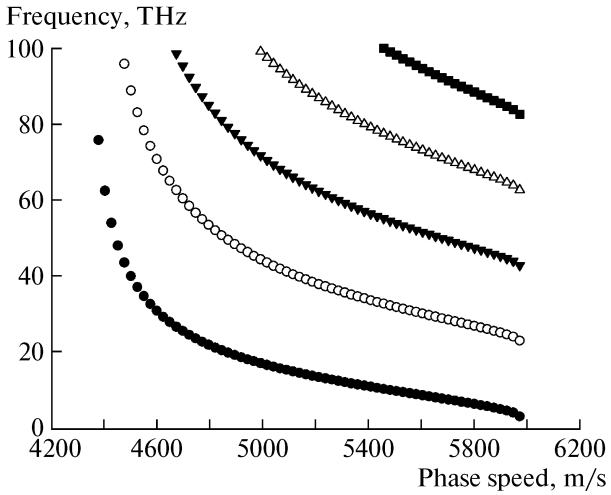

Fig. 4. Dispersion curves for a two-layered nanocomposite in contact with the half-space; the external layer has a thickness of 10 nm, internal layer, 1 nm.

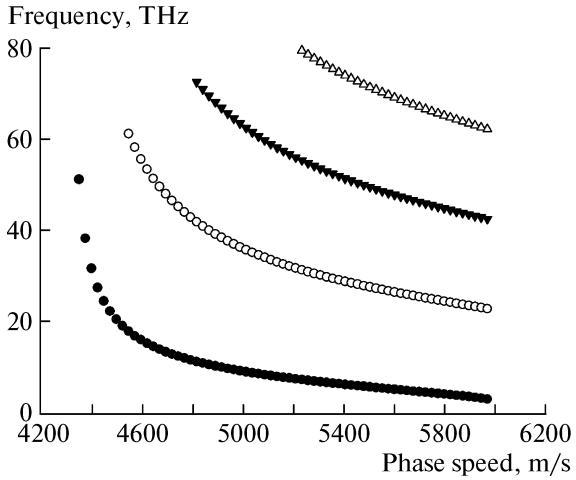

Fig. 5. Dispersion curves for a two-layered nanocomposite in contact with the half-space; the external layer has a thickness of 1 nm, internal layer, 10 nm.

noted above, in crystalline media waves with frequencies higher than 4–5 THz are impossible.

Figure 5 shows the dispersion curves for a similar composite with 1-nm upper and 10-nm lower layers.

Figure 6 shows the lower branches of dispersion curves for the composite considered in the first example (external 10-nm and internal 1-nm layers) for varying thickness of the internal layer.

These data demonstrate that Love waves are informative and provide investigation of the change of geometry of the internal nanolayer using corresponding dispersion curves. Similar data are available for the variation of elastic properties of the internal layer.

7.2. SH Waves in Multilayered Media

The multilayered plate with free surfaces consisting of 31 isotropic layers with the following properties is considered:

$$E_{2n+1} = 1, \quad \rho_{2n+1} = 1, \quad h_{2n+1} = 1,$$

$$E_{2n} = 4, \quad \rho_{2n1} = 1, \quad h_{2n} = 1.$$

The method of high accuracy calculations was used for solution of this problem (calculations were performed with numbers that had more than 1000 decimal digits). Figure 7 shows the first 25 dispersion curves for SH waves propagating in this plate.

In this figure two facts should be pointed out: the occurrence of the lower dispersion curve corresponding to SH waves propagating with frequencies close to

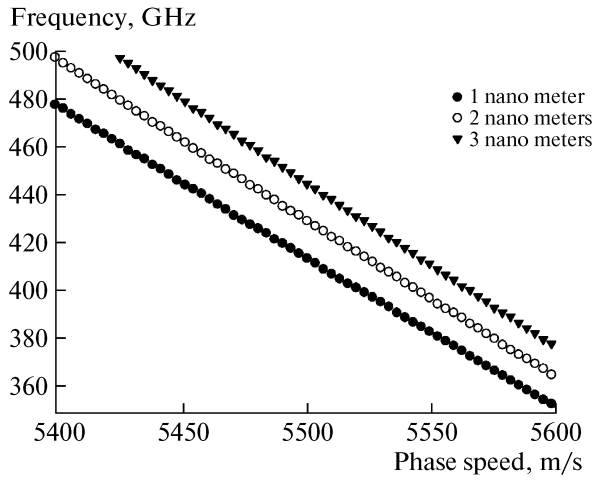

Fig. 6. Lower branches of dispersion curves for varying thickness of the internal layer.

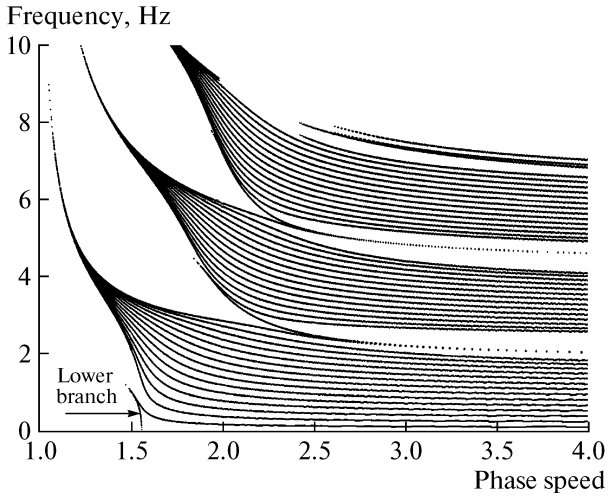

Fig. 7. First 25 dispersion curves for a 31-layered plate.

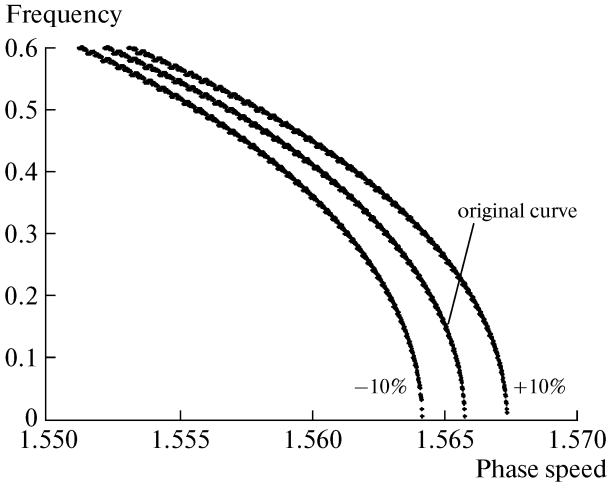

Fig. 8. Change of lower branch of dispersion curves for a 31-layer plate for varying thickness of the middle layer.

zero and unlimited range of phase velocities (unlike Love waves whose velocities are limited).

It is interesting to note that, even for such a large number of layers, the lower dispersion curve turns out to be informative. For example, change of thickness of the middle layer by 10% results in noticeable change of the lower branch (see Fig. 8).

In conclusion, it should be noted that the boundary acoustic waves widely used in acoustoelectronics [68] are applied not only for diagnostics of layered composites, but in many other diagnostic problems as well. These problems have more than once been discussed in *Acoustical Physics* (see, e.g., [69–79]).

ACKNOWLEDGMENTS

This work was supported by the Russian Foundation for Basic Research, project no. 09-01-12063.

REFERENCES

1. R. V. Goldstein, A. V. Kaptsov, and S. V. Kuznetsov, in *Actual Problems of Mechanics* (Nauka, Moscow, 2009), pp. 56–75 [in Russian].
2. A. E. H. Love, *Some Problems of Geodynamics* (Cambridge Univ., London, 1911).
3. G. Kol'sky, *Stress Waves in Elastic Bodies* (Inostr. Liter., Moscow, 1955) [in Russian].
4. D. Achenbach, J. Acoust. Soc. Am. **103**, 2283 (1998).
5. E. Dieulesaint and D. Royer, *Elastic Waves in Solids* (Wiley, New York, 1980).
6. R. A. Kline, *Nondestructive Characterization of Composite Media* (Technomic, Lancaster, PA, 1991).
7. R. A. Kline and Z. T. Chen, in *Materials Evaluation* (1988), pp. 986–992.
8. R. Kline, L. Jiang, and E. Drescher-Krasicka, Rev. Progress in QNDE, p. 1907 (1995).
9. M. A. Doxbeck, M. A. Hussain, J. Rama, A. Abate, and J. Frankel, Rev. Progress in QNDE **21**, 292 (2002).
10. S. V. Kuznetsov, Q. Appl. Math. **62** (2004).
11. N. A. Haskell, Bull. Seism. Soc. Am. **43**, 17 (1953).
12. W. T. Thomson, J. Appl. Phys. **21**, 89 (1950).
13. L. Knopoff, Bull. Seism. Soc. Am. **54**, 431 (1964).
14. A. K. Mal and L. Knopoff, J. Math. Anal. Appl. **21**, 431 (1968).
15. M. Mallah, L. Philippe, and A. Khater, Comp. Mater. Sci. **15**, 411 (1999).
16. A. Elbahrawy, J. Acoust. Soc. Am. **96**, 3155 (1994).
17. O. I. Lobkis and D. E. Chimenti, J. Acoust. Soc. Am. **102**, 143 (1997).
18. Y. B. Chastel and P. R. Dawson, J. Geophys. Res. **98**, 757 (1993).
19. A. K. Mal, Geophys. Appl. **51**, 47 (1962).
20. K. L. McLaughlin, T. G. Barker, S. M. Day, B. Shkoller, and J. L. Stevens, J. Geophys. Int. **111**, 291 (1992).
21. E. Penttila, Geophys., p. 7 (1960).
22. F. Simons, A. Zielhuis, and V. D. Hilst, Lithos. **48**, 17 (1999).

23. B. L. N. Kennett, J. Geophys. Int. **122**, 470 (1995).
24. B. L. N. Kennett, J. Geophys. Int. **133**, 159 (1998).
25. Y.-S. Zhang and T. Tanimoto, Phys. Earth Planet. Inter. **66**, 160 (1991).
26. W. Yang and T. Kundu, J. Eng. Mech. ASCE **124**, 311 (1998).
27. H. Lamb, Philos. Trans. R. Soc. London A **203**, 1 (1904).
28. H. Lamb, Proc. R. Soc. A **93**, 114 (1917).
29. L. M. Brekhovskikh, *Waves in Layered Media* (Nauka, Moscow, 1973; Academic, New York, 1980).
30. S. V. Kuznetsov, Q. Appl. Math. **60**, 587 (2002).
31. A. L. Shuvalov, Proc. R. Soc. A **456**, 2197 (2000).
32. M. J. S. Lowe, IEEE Trans. Ultrason. Ferroelectr. Freq. Control **42**, 525 (1995).
33. S. G. Lekhnitskii, *Anisotropic Plates* (Gordon Breach, New York, 1949).
34. R. D. Mindlin, in *Structural Mechanics*, Ed. by J. N. Goodier and J. N. Hoff (Pergamon, New York, 1960), pp. 199–232.
35. E. G. Newman and R. D. Mindlin, J. Acoust. Soc. Am. **29**, 1206 (1957).
36. E. L. Adler, IEEE Trans. Ultrason. Ferroelectr. Freq. Control **37**, 485 (1990).
37. E. L. Adler, J. Slaboszewicz, G. W. Farnell, and C. K. Jen, IEEE Trans. Ultrason. Ferroelectr. Freq. Control **37**, 215 (1990).
38. A. H. Fahmi and E. L. Adler, Appl. Phys. Lett. **22**, 495 (1973).
39. V. Dayal and V. K. Kinra, J. Acoust. Soc. Am. **85**, 2268 (1989).
40. V. Dayal and V. K. Kinra, J. Acoust. Soc. Am. **89**, 1590 (1991).
41. M. Nakahata, IEEE Trans. Ultrason. Ferroelectr. Freq. Control **42**, 362 (1995).
42. T. C. T. Ting and P. Chadwick, in *ASME Symp. on Wave Propagation in Structural Composites*, Ed. by A. K. Mal and T. C. Ting, **90**, 69 (1988).
43. A. Safaeinili, D. E. Chimenti, B. A. Auld, and S. K. Datta, Composites Eng. **5**, 1471 (1995).
44. J. Park, J. Geophys. Int. **126**, 173 (1996).
45. C. Potel et al., J. Appl. Phys. **86**, 1128 (1999).
46. J. W. Strutt, Proc. London Math. Soc. **17**, 4 (1885).
47. I. A. Viktorov, *Rayleigh and Lamb Waves: Physical Theory and Applications* (Plenum, New York, 1967; Nauka, Moscow, 1967).
48. M. Rahman and J. R. Barber, J. Appl. Mech. Trans. ASME **62**, 250 (1995).
49. D. Achenbach, *Wave Propagation in Elastic Solids* (North-Holland, Amsterdam, 1975).
50. V. G. Mozhaev, Sov. Phys. Acoust **37**, 186 1991).
51. D. Royer and E. Dieulesaint, J. Acoust. Soc. Am. **76**, 1438 (1985).
52. G. W. Farnell, Phys. Acoust. **6**, 109 (1970).
53. A. N. Stroh, J. Math. Phys. **41**, 77 (1962).
54. D. M. Barnett and J. Lothe, Phys. Norv. **7**, 13 (1973).
55. D. M. Barnett and J. Lothe, J. Phys. Ser. F **4**, 671 (1974).
56. D. M. Barnett and J. Lothe, J. Phys. Ser. F **4**, 1618 (1974).
57. P. Chadwick and G. D. Smith, Adv. Appl. Mech. **17**, 303 (1977).
58. P. Chadwick and D. A. Jarvis, Proc. R. Soc. London A **366**, 517 (1979).
59. T. C. T. Ting, Proc. R. Soc. London A **453**, 449 (1997).
60. T. C. T. Ting and D. M. Barnett, Wave Motion **26**, 207 (1997).
61. S. V. Kuznetsov, J. Multiscale Comp. Eng. **1**, 57 (2002).
62. S. V. Kuznetsov, Q. Appl. Math. **61**, 575 (2003).
63. S. V. Kuznetsov, Q. Appl. Math. **60**, 87 (2002).
64. D. Alleyne and P. Cawley, Rev. Progress in QNDE **13**, 181 (1994).
65. R. A. Kline, R. E. Green, and C. H. Palmer, J. Appl. Phys., 141 (1981).
66. R. C. Addison and A. D. W. McKie, Rev. Progress in QNDE **14**, 521 (1995).
67. Y. Nagata, J. Huang, J. D. Achenbach, and S. Krishnaswamy, Rev. Progress in QNDE **14**, 561 (1995).
68. Yu. V. Gulyaev and F. S. Hickernell, Akust. Zh. **51**, 101 (2005) [Acoust. Phys. **51**, 81 (2005)].
69. I. V. Anisimkin, Akust. Zh. **50**, 442 (2004) [Acoust. Phys. **50**, 370 (2004)].
70. I. V. Anisimkin, Akust. Zh. **50**, 149 (2004) [Acoust. Phys. **50**, 115 (2004)].
71. V. V. Kozachenko and I. Ya. Kucherov, Akust. Zh. **50**, 231 (2004) [Acoust. Phys. **50**, 185 (2004)].
72. B. D. Zaitsev, I. E. Kuznetsova, and I. A. Borodina, Akust. Zh. **50**, 462 (2004) [Acoust. Phys. **50**, 388 (2004)].
73. N. L. Batanova, A. V. Golenishchev-Kutuzov, V. A. Golenishchev-Kutuzov, and R. I. Kalimullin, Akust. Zh. **50**, 585 (2004) [Acoust. Phys. **50**, 496 (2004)].
74. M. Yu. Dvoesherstov, V. I. Cherednik, and A. P. Chirimanov, Akust. Zh. **50**, 603 (2004) [Acoust. Phys. **50**, 512 (2004)].
75. I. V. Anisimkin, V. I. Anisimkin, Yu. V. Gulyaev, and E. Verona, Akust. Zh. **48**, 12 (2002) [Acoust. Phys. **48**, 8 (2002)].
76. V. V. Tyutekin, Akust. Zh. **52**, 847 (2006) [Acoust. Phys. **52**, 733 (2006)].
77. A. I. Korobov and M. Yu. Izosimova, Akust. Zh. **52**, 683 (2006) [Acoust. Phys. **52**, 589 (2006)].
78. O. S. Tarasenko, S. V. Tarasenko, and V. M. Yurchenko, Akust. Zh. **52**, 539 (2006) [Acoust. Phys. **52**, 462 (2006)].
79. M. Yu. Izosimova, A. I. Korobov, and O. V. Rudenko, Akust. Zh. **55**, 153 (2009) [Acoust. Phys. **55**, 153 (2009)].